THE CFD MODELING OF TWO-DIMENSIONAL TURBULENT MHD CHANNEL FLOW

by

Živojin M. STAMENKOVIĆ*, Miloš M. KOCIĆ, and Jelena D. PETROVIĆ

Hydro Energy Department, Faculty of Mechanical Engineering,
University of Niš, Niš, Serbia

Original scientific paper
https://doi.org/10.2298/TSCI160822093S

In this paper, influence of magnetic field on turbulence characteristics of two-dimensional flow is investigated. The present study has been undertaken to understand the effects of a magnetic field on mean velocities and turbulence parameters in turbulent 2-D channel flow. Several cases are considered. First laminar flow in a channel and MHD laminar channel flow are analyzed in order to validate model of magnetic field influence on electrically conducting fluid flow. Main part of the paper is focused on MHD turbulence suppression for 2-D turbulent flow in a channel and around the flat plate. The simulations are performed using ANSYS CFX software. Simulations results are obtained with BSL Reynolds stress model for turbulent and MHD turbulent flow around flat plate. The nature of the flow has been examined through distribution of mean velocities, turbulent fluctuations, vorticity, Reynolds stresses and turbulent kinetic energy.

Key words: *turbulence, magnetohydrodynamics, suppression, CFD*

Introduction

The research of wall-bounded turbulent flows is of a significant importance in practical engineering applications such as turbine blade internal cooling, advanced gas-cooled nuclear reactors, heat exchangers and cooling of microelectronic devices. For instance, research conducted to date of turbulent channel flow has proven to be an extremely useful framework for the study of turbulence and possibility of turbulence suppression and for the basic understanding of internal shear flows. Also the channel flow is one of the most easily reproducible flows in the laboratory for fundamental research and for many industrial applications. Therefore, these classical types of flows have attracted the attention of a large number of fluid mechanics researchers, utilizing both experimental and numerical approaches.

One of the first experimental investigations with detailed turbulence measurements of a fully developed turbulent flow in a channel bounded by flat plates was done by Laufer [1], Comte-Bellot [2], and Clark [3]. Turbulent flow in smooth and rough tubes and channels has been studied intensively during the last century, and to this day are continued with undiminished interest. For example, with fuel being the second highest cost category after

* Corresponding author, e-mail: zikas@masfak.ni.ac.rs

personnel at most airlines [4] its efficient use has become the dominant issue. The technological goals inspired by ecological and economical considerations can be met by improving energy sources, engines, aircraft weight, and air drag. Of the latter, approximately 50% are caused by skin friction [5]. This percentage is unlikely to decrease in the near future as to date no technologies are available to substantially lower the wall shear stress on commercial airplanes. However, in the case of very low Reynolds numbers, numerical studies of turbulent channel flow have shown that a reduction in drag is possible.

Reynolds-Averaged Navier-Stokes (RANS) simulations are widely used to optimize various industrial turbulent and laminar flows because of their low computational cost. However, it is well-known that accuracy of these CFD simulations in complex flows is limited by the difficulties in modeling the complex turbulence interactions through transport equations for the mean flow variables [6]. A large number of researchers have made a great effort to date to validate, improve and custom tailor models of turbulent flows for different classes of flows [7-9].

Beside the experimental turbulent flows research, numerical analysis of turbulent flows and development of turbulent models significant effort have been devoted to the control of turbulent flows. The active control of turbulent flows is gaining recognition as a possible means for greatly improved performance of aerospace and marine vehicles [10]. While passive devices have been used effectively in the past, active control strategies have the potential of allowing a significant improvement in the performance of future configurations. Choi *et al*. [11] first introduced active feedback turbulent flow control.

The MEMS technology offers the potential for the large-scale active control of coherent flow structures within the boundary layer. This could lead to the reduction of skin friction drag or the postponement of flow separation using *smart skins* capable of detecting and reacting to the state of the local boundary layer [12].

During the last decade, emphasis has been on the development of active control methods in which energy, or auxiliary power, is introduced into the flow. One of the active control methods is MHD control. If a fluid is electrically conducting, electromagnetic flow control permits to act directly within the boundary layer by applying directly local Lorentz forces.

The Lorentz forces arising from the induced currents in the conducting liquid lead to additional Joule dissipation and tend to suppress gradients along the direction of the magnetic field. In certain cases may be encountered the laminar or transitional flow which for some characteristic values of hydraulic parameters in the case of non-conducting fluid would already be in distinctly turbulent motion.

Static magnetic fields are often used nowadays for flow control in metallurgy [13], crystal growth [14], liquid metal flows in fusion reactor blankets [15]. Previous application of magnetic field to transition to turbulence in a case of electrically conducting fluid flow is clearly a relevant problem from a practical point of view. It is also of interest in the general context of shear flow transition because the magnetic field may modify the mechanisms that have been identified as important in subcritical transition of non-conducting shear flows. The main effect of the Lorentz force that results from the induced electric currents is then to diffuse momentum along the magnetic field lines. Flow structures tend to become elongated along this direction and even invariant if this effect is not effectively opposed by inertia or viscosity [16].

Research in this paper is motivated by several experimental and numerical investigations conducted in the field of MHD channel flow. Beside the experimental investigations presented by Henoch and Stace [17] and Weier *et al*. [18], special attention is paid to work of Branover *et al*. [19] in which experimental results of turbulence suppression in rectangular channel with 2.8 × 5.6 cm^2 cross section with uniform magnetic field directed normal to the longer side of the channel cross section are presented.

Branover *et. al*. [19] performed experiments mainly at mean velocity U = 0.16 m/s corresponding to Reynolds number Re = 52 · 10^3, while Hartmann number varied in the range 60-1200, and interaction parameter varied in the range of 0.15-0.27. MHD experiments in transverse magnetic field have revealed a significant turbulence intensity u'/U dependence on its value. Turbulence intesity decreases under a comparatively weak magnetic field increasing in the range of $0 < 10^3$ Ha/Re < 2.5.

Other mentioned MHD experiments in salt water has demonstrated drastic alterations of a turbulent boundary layer under the influence of MHD force. The documented effects range from a reduction in streamwise turbulent fluctuations to an extensive stretching and thinning of the boundary layer.

Besides the listed experimental research a special motivation to research presented in this paper provide the work Smolentsev and Moreau [20]. Their study is motivated by the need for developing turbulence models for quasi-two-dimensional MHD turbulent flow in the channel for fusion applications.

The present study have been undertaken to understand the effects of a magnetic field on turbulence parameters of 2-D channel flow. First the BSL Reynolds stress model is extended in order to add magnetic field influence on electrically conducting fluid flow and to validate the model and second part of the paper is focused on MHD turbulence suppression for two-dimensional turbulent flow in a channel and around the flat plate. The simulations are performed using ANSYS CFX solver.

In addition to the mentioned papers is important to mention that the research in this field published by other authors [21-24] are very important for the analysis of the effect of magnetic field on the turbulent flow.

Physical, turbulent model and numerical grid

We consider the MHD turbulent flow of an incompressible electrically conducting fluid in an plane channel between two perfectly insulating walls located at $y = 0$ and $y = h$, and around the flat plate in the same channel, where x, y, z denote the streamwise, wall-normal and spanwise directions, respectively. The flow is driven by a variable pressure gradient providing constant volume flux and subjected to a uniform magnetic field vector $\mathbf{B} = B\mathbf{e}$, where $\mathbf{e}$ = (0,-1,0). The geometry is sketched in fig. 1.

The MHD flows in a blanket are characterized by four dimensionless parameters: the magnetic Reynolds number, Hartmann number, Reynolds number, and the wall conductance ratio c_w.

$$\mathrm{Re_m} = \mu_0 \sigma U h\,,\ \mathrm{Ha} = Bh\sqrt{\frac{\sigma}{\rho \nu}}\,,\ \mathrm{Re} = \frac{Uh}{\nu}\,,\ c_w = \frac{t_w \sigma_w}{h\sigma} \tag{1}$$

Here, B, h, and U are the applied magnetic field intensity, characteristic cross sectional dimension, and the mean-flow velocity, while μ_0, t_w, σ_w, ρ, ν, and σ are the magnetic permeability, wall thickness, wall electrical conductivity, fluid density, kinematic viscosity, and the fluid electrical conductivity correspondingly. The MHD flow in the channel is analyzed for chemical solution whose electrical conductivity of the order of $\sigma \sim 10^2$.

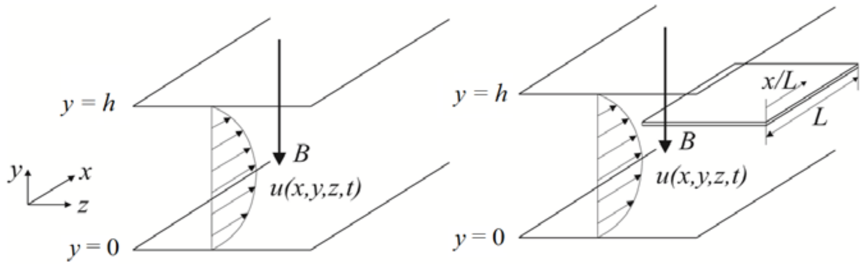

Figure 1. Physical model of considered cases

The Reynolds number has a value of 620 in the case of laminar flow, while for the turbulent flow order of Reynolds number is Re = $31 \cdot 10^3$. On the contrary, the magnetic Reynolds number Re_m in the blanket flows is much smaller than unity, so that the induced magnetic field is negligibly smaller than the applied one. For the considered cases Hartamnn number Ha varies in the range from 5 to 80. This parameter plays an important role in MHD wall-bounded flows, where the thickness of the MHD boundary layer at the walls perpendicular to the magnetic field is proportional to 1/Ha. In particular, it implies that the key parameter in modeling MHD turbulence is the ratio Re/Ha.

In a homogeneous magnetic field, turbulence is precisely determined by the antagonism between the inertia and Lorentz force and by the interaction parameter $N = \mathrm{Ha}^2/\mathrm{Re} = \sigma B^2 h/(\rho U)$, which represents their ratio. This study is limited to the particular case of insulating walls, *i. e.*, $c_w = 0$.

The channel height is $h = 0.028$ m in accordance with Branover experiment and the channel length is 2 m. According to the Branover experiment the channel has a width much greater than height h, so that the system can be considered 2-D. In accordance with this conclusion, symmetry boundary conditions were applied for the planes in the spanwise direction.

For all considered case at the inlet of domain, uniform velocity field is defined. Domain is meshed with structured hexahedral mesh with 1200 uniform spaced cells in flow direction and in direction normal the Hartman walls there is 160 cells densely spaced along the walls of the channel in order to obtain the value of y^+ equal to one, while in spanwise direction symmetry boundary conditions have been applied. Meshed domains are represented at fig. 2.

The considered flow domain has a length of 2 m (divided to 1200 cells), a height of 0.028 m (with 160 cells), while in spanwise direction symmetry boundary conditions have been applied. All simulations were performed with uniform inlet velocity, atmospheric pressure at outlet, no slip walls, and two symmetry boundaries in z direction. Walls are non conducting, magnetic field is applied in negative y direction, while in the case of flow around the flat plate (which have 1 mm thickness and 100 mm length), number of cells in y directions is increased to 180. Mesh is densely spaced along the walls of the channel and around the flat plate in order to obtain the value of y^+ equal to one.

In this study, it assumed that fluid is incompressible and electrically conducting. The governing equations are the mass and momentum conservations.

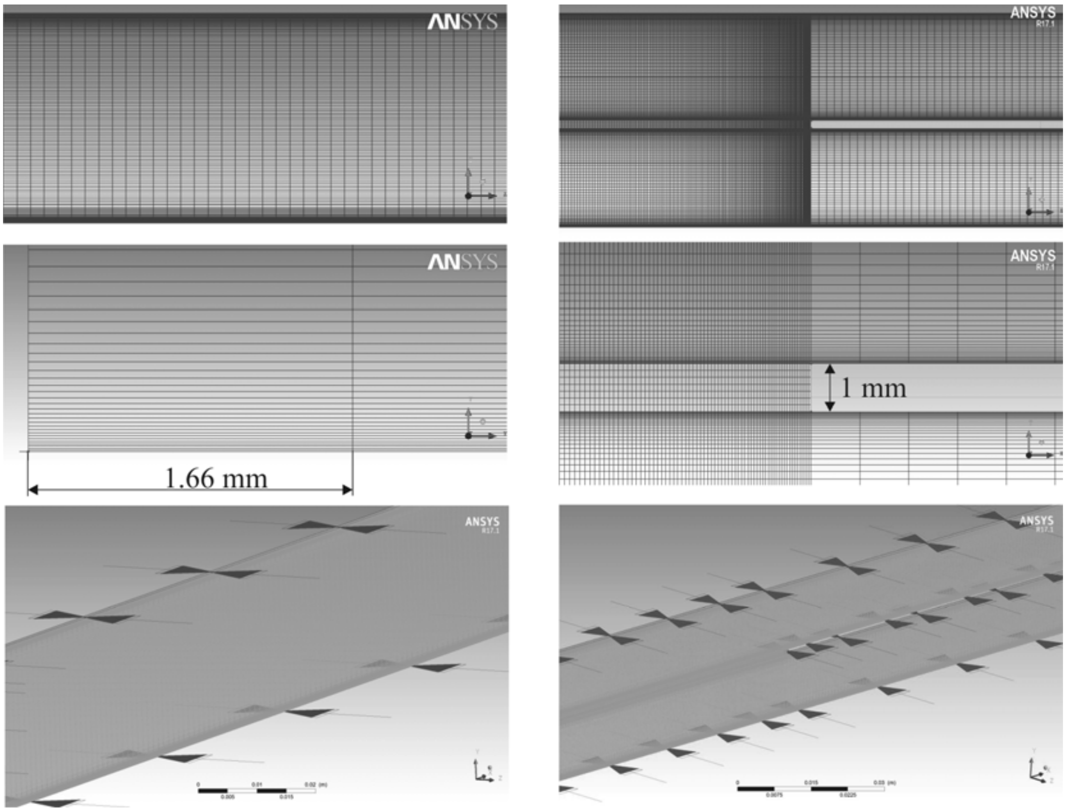

Figure 2. Mesh of computational domains (left-flow domain, right-flow domain with flat plate)
(for color image see journal website)

Using the Reynolds averaging approach, the averaged Navier-Stokes equation can be stated as:

$$\frac{\partial u_i}{\partial x_i} = 0 \tag{2}$$

$$\frac{\partial}{\partial t}\left(\rho u_i\right) + \frac{\partial}{\partial x_j}\left(\rho u_i u_j\right) = -\frac{\partial p}{\partial x_i} + \frac{\partial}{\partial x_j}\left[\mu\frac{\partial u_i}{\partial x_j} - \rho\overline{u_i' u_j'}\right] + \mathrm{f}_{Li} \tag{3}$$

where $-\rho\overline{u_i' u_j'}$ represents Reynolds stresses and f_L is Lorentz body force included in momentum equation for MHD flow.

Since magnetic Reynolds number ($\mathrm{Re_m}$) is less than unity in considered case, the induced magnetic field due to the induced electric current can be neglected. After neglecting the induced magnetic field, the electric potential method can be used to determine the current and the Lorentz force by the following equations:

$$\vec{\mathrm{f}}_L = \vec{\mathrm{j}} \times \vec{\mathrm{B}} \tag{4}$$

$$\vec{\mathrm{j}} = \sigma\left(-\nabla\phi + \vec{\mathrm{u}} \times \vec{\mathrm{B}}\right) \tag{5}$$

$$\nabla \cdot \vec{\mathrm{j}} = 0 \tag{6}$$

The Reynolds-averaged approach to turbulence modeling reuires that the Reynolds stresses in the eq. (3) are appropriately modeled. Boussinesq relates the Reynolds stress with mean strain-rate tensor by the dynamic eddy-viscosity μ_t according to the following equation:

$$-\rho\overline{u_i' u_j'} = \mu_t\left(\frac{\partial u_i}{\partial x_j} + \frac{\partial u_j}{\partial x_i}\right) - \frac{2}{3}\left(\rho k + \mu_t \frac{\partial u_k}{\partial x_k}\right)\delta_{ij} \tag{7}$$

In this paper, the two equation BSL Reynolds stress turbulence model is used for modeling turbulent viscosity. The turbulence kinetic energy k and the specific dissipation rate ω, with the magnetic field influnce, are obtained from the following transport equations:

$$\frac{\partial}{\partial t}(\rho k) + \frac{\partial}{\partial x_i}(\rho k u_i) = \tau_{ij}\frac{\partial u_j}{\partial x_i} - \beta\rho k\omega + \frac{\partial}{\partial x_i}\left[(\mu + \sigma_k \mu_t)\frac{\partial k}{\partial x_i}\right] - 2\alpha_m k\sigma B^2 \tag{8}$$

$$\begin{aligned}\frac{\partial}{\partial t}(\rho\omega) + \frac{\partial}{\partial x_i}(\rho\omega u_i) &= \frac{\gamma}{\nu_t}\tau_{ij}\frac{\partial u_j}{\partial x_i} - \beta\rho\omega^2 + \frac{\partial}{\partial x_i}\left[(\mu + \sigma_\omega \mu_t)\frac{\partial \omega}{\partial x_i}\right] + \\ &+ 2\rho(1 - F_1)\sigma_{\omega 2}\frac{1}{\omega}\frac{\partial k}{\partial x_i}\frac{\partial \omega}{\partial x_i} - \alpha_m \omega\sigma B^2.\end{aligned} \tag{9}$$

The blending function F_1 was designed to be one in sublayer and logarithmic region of the boundary layer and to gradually approach zero in the wake region. This means that the new model is based on the k-ω formulation, with the original Wilcox model activated in the near wall region and the standard k-ε model activated in the outer wake region and in free shear layers. This first step leads to a new model that will be termed the baseline (BSL) model. The BSL model has a performance very similar to that of the original k-ω model, but without the undesirable freestream dependency [25].

Test cases

The present problem of flow is considered for four basic cases, as follows: laminar flow, laminar MHD flow, turbulent flow and turbulent MHD flow.

The first two flow regimes have their own analytic solutions [26] for considered cases which are determined for defined boundary conditions in the following forms:

$$u = \frac{1}{2}\frac{1}{\mu}\frac{\mathrm{d}p}{\mathrm{d}x}\left(y^2 - hy\right) \tag{10}$$

$$u(y) = \frac{1}{\mu}\frac{\mathrm{d}p}{\mathrm{d}x}\frac{h^2}{\mathrm{Ha}^2}\left[\left(\frac{1 - \cosh(\mathrm{Ha})}{\sinh(\mathrm{Ha})}\right)\sinh\left(\frac{\mathrm{Ha}}{h}y\right) + \cosh\left(\frac{\mathrm{Ha}}{h}y\right) - 1\right] \tag{11}$$

The obtained numerical simulations results were compared with analytical solutions as to validate the model in ANSYS CFX software, which defines the influence of magnetic fields on the flow of electrically conducting fluid. The results are shown in figs. 3 and 4, a match the results obtained are very satisfactory. The 2-D MHD flow problem of electrically conducting fluid in a rectangular duct subject to a uniform transverse magnetic field is the recommended benchmark.

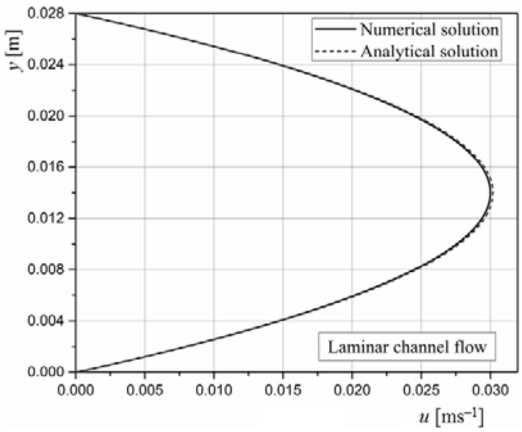

Figure 3. Laminar flow velocity distribution

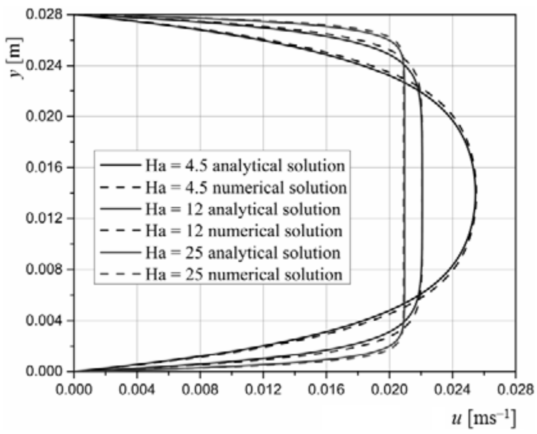

Figure 4. The MHD Laminar flow velocity distribution *(for color image see journal website)*

Part of obtained results for laminar MHD flow is shown in figs. 5 and 6. At the fig. 5 the shear strain rate and at the fig. 6 the vorticity for laminar and MHD laminar flow in channel is presented. The strain rate tensor is defined by:

$$S_{ij} = \frac{1}{2}\left(\frac{\partial u_i}{\partial x_j} + \frac{\partial u_j}{\partial x_i}\right) \tag{12}$$

This tensor has three scalar invariants, one of which is often simply called the shear strain rate:

$$II_S = \left(2\frac{\partial u_i}{\partial x_j}S_{ij}\right)^{0.5} \tag{13}$$

with 2-D velocity components u,v, this expands to:

$$II_S = \left[2\left\{\left(\frac{\partial u}{\partial x}\right)^2 + \left(\frac{\partial v}{\partial y}\right)^2\right\} + \left(\frac{\partial u}{\partial y} + \frac{\partial v}{\partial x}\right)^2\right]^{0.5} \tag{14}$$

Obtained results show that with increasing Hartmann number, shear strain rate and vorticity significantly reduce through the entire channel height except in areas close to the walls where the intensity increases significantly.

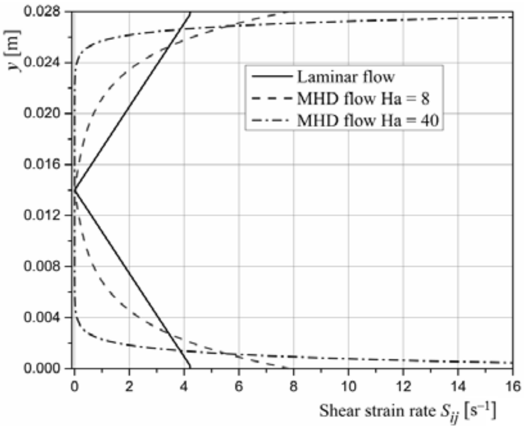

Figure 5. Influence of Hartmann number on shear strain rate

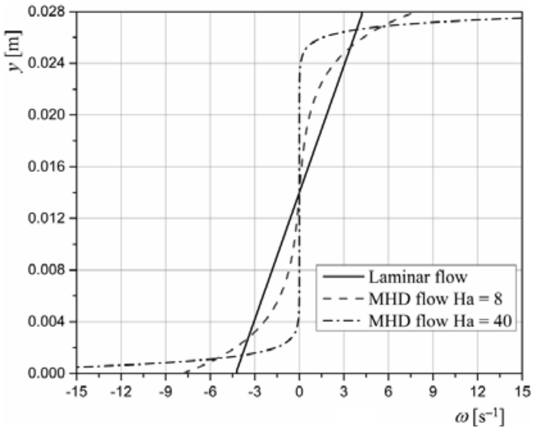

Figure 6. Influence of Hartmann number on vorticity

Turbulent MHD channel and flat plate flow

In this section, we study the properties of a turbulent duct flow in the presence of a uniform wall normal magnetic field at low magnetic Reynolds numbers $\mathrm{Re_m} \ll 1$ and at moderate hydrodynamic Reynolds number $\mathrm{Re} = 31 \cdot 10^3$. We study the effect of magnetic field on the evolution of turbulence and characteristic properties of turbulent flow at relatively low Hartmann number. The aim of this study is to obtain a sense of the impact of magnetic field on turbulent Hartmann duct flow.

Velocity components in longitudinal and transversal directions (u, v) for turbulent channel flow in the presence or absence of magnetic field influence are shown at the figs. 7 and 8. Increasing the Hartmann number does not give significant changes for velocity component in the direction of flow. Similar to the laminar flow velocity gradient near the walls of the channel becomes steeper while in the rest of the channel velocity field becomes uniform.

In the case of transverse velocity component, the effect of magnetic field is opposite, namely the velocity gradients near the walls of the channel are reduced, as well as the intensity of the velocity component over the entire height of the channel.

Usual analysis of turbulent flow starts with decomposition of the flow into its mean and fluctuating components. By applying this decomposition to the transport equations of momentum and kinetic energy some of the mechanisms by which turbulence affects the mean flow can be isolated. This is the main reason that in figs. 9 and 10 the influence of magnetic field on the change of the turbulent kinetic energy and Reynolds stress tensor component $\overline{u'v'}$ is presented. From the figures it is clear that increasing of Hartmann number reduces the turbulent kinetic energy and Reynolds stresses, which is especially noticeable in the middle of the channel.

The Reynolds stress terms play a pivotal role in turbulence production. Physically, correlations between fluctuating velocity components u', v' represents the mean value of the transport of fluctuating momentum by the fluctuating velocity field. Transport of fluctuating momentum influences the transport of the mean momentum, so this correlation can therefore be interpreted as a mechanism for momentum exchange between the mean flow and the turbulence.

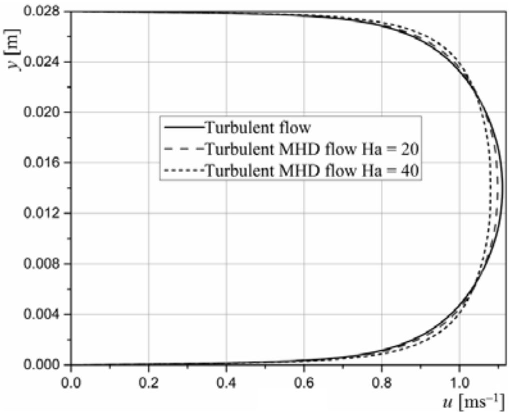

Figure 7. Influence of Hartmann number on longitudinal velocity component

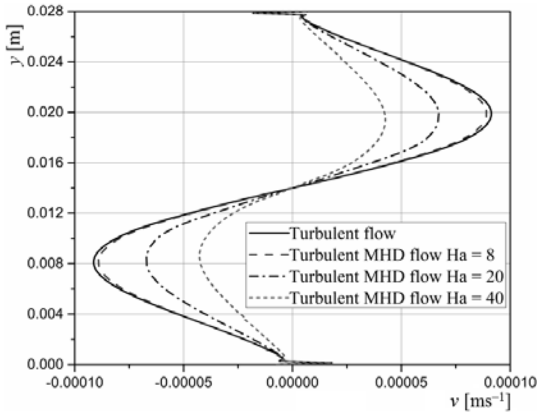

Figure 8. Influence of Hartmann number on transverse velocity component

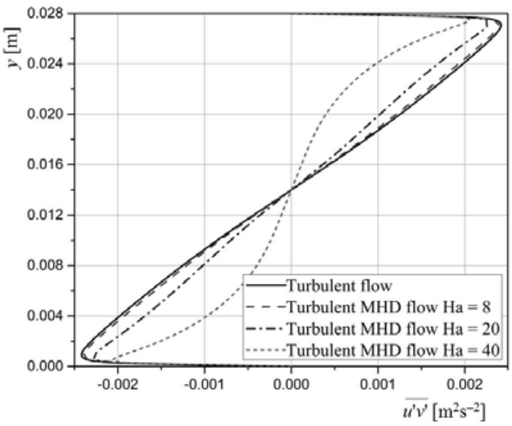

Figure 9. Influence of Hartmann number on Reynolds stress component $\overline{u'v'}$

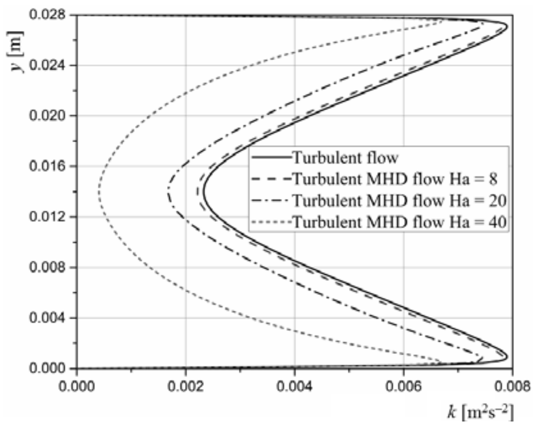

Figure 10. Influence of Hartmann number on turbulent kinetic energy

Obtained result shows the significant reduction of turbulent kinetic energy and Reynolds stresses especially in the core flow region. As a result of magnetic field *i. e*. Lorentz force the fluctuating components of velocity are suppressed and consequently turbulence kinetic energy is reduced and also turbulent vertical advection of streamwise turbulent momentum $u'v'$, or more simply the vertical flux of streamwise momentum.

The CFD simulation results of quasi-static MHD flow indicate that the Hartmann flow has two opposing effects namely the Hartmann flattening and turbulence suppression effects. These effects can also be used to reduce skin friction. An initial increase in skin friction coefficient can be expected due to the Hartmann flattening, which is followed by a decrease in skin friction (wall shear) when suppression of turbulence becomes important. In order to further analysis of these results and more detailed research of the magnetic fields effects on the boundary layer flow, the flow around a thin flat plate in the same channel in the presence of perpendicular magnetic field is considered.

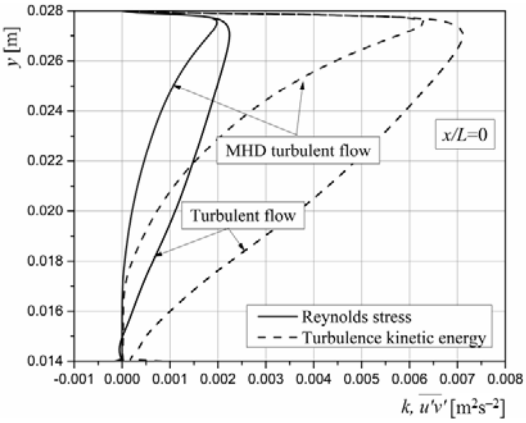

Figure 11. Influence of magnetic field on turbulent kinetic energy and Reynolds stresses (*x/L* = 0) *(for color image see journal website)*

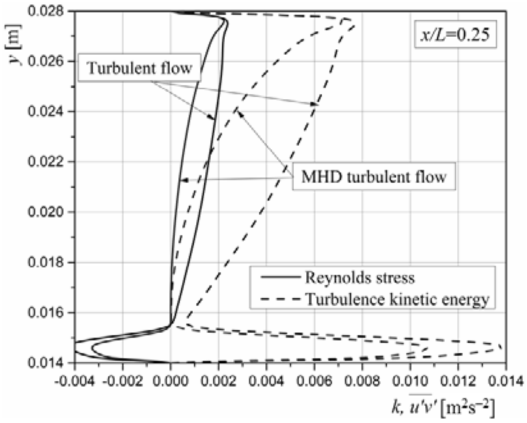

Figure 12. Influence of magnetic field on turbulent kinetic energy and Reynolds stresses (*x/L* = 0.25) *(for color image see journal website)*

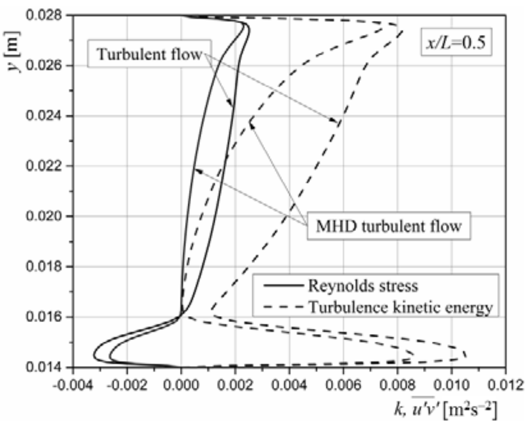

Figure 13. Influence of magnetic field on turbulent kinetic energy and Reynolds stresses (*x/L* = 0.5) *(for color image see journal website)*

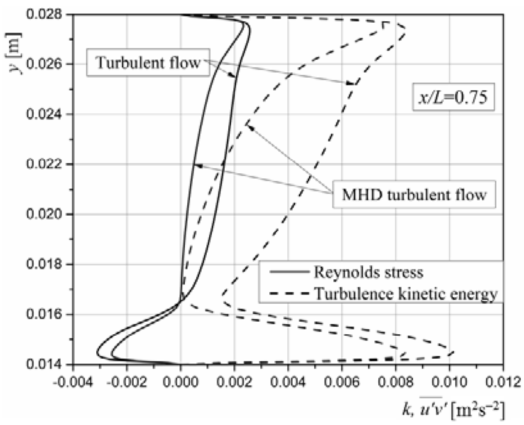

Figure 14. Influence of magnetic field on turbulent kinetic energy and Reynolds stresses (*x/L* = 0.75) *(for color image see journal website)*

A MHD force, when applied to an electrically conducting fluid, can increase the near wall velocity, decrease the boundary layer thickness and suppress the intensity of the turbulent fluctuations across the boundary layer. Some research results indicate that fluctuating wall shear stress and turbulence intensity can be suppressed up to 30%.

In figs. 11-14 the distribution of turbulent kinetic energy and Reynolds stress component $\overline{u'v'}$ for the region from the flat plate to the upper wall of the channel has been presented. The figures show different positions along the flat plate whereby $x/L = 0$ corresponds to the beginning of the flat plate, and $x/L = 1$ its end. The obtained results are compared for flow in the absence of a magnetic field and for MHD turbulent flow in which the Hartmann number is equal to 40.

All the results show a decrease in the intensity of the turbulent kinetic energy and Reynolds stresses, but it is interesting to note that this reduction for considered flow problem is greater in the primary stream compared to the boundary layer.

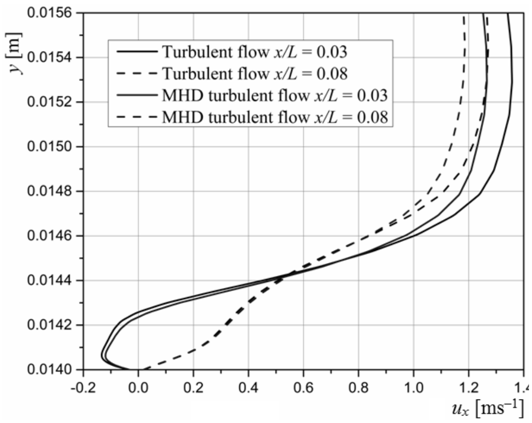

Figure 15. Boundary layer velocity for turbulent and MHD turbulent flow *(for color image see journal website)*

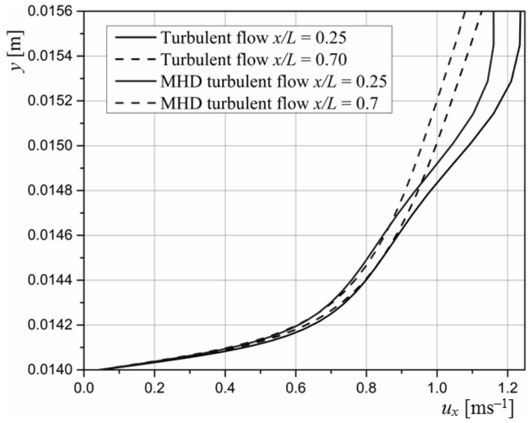

Figure 16. Boundary layer velocity for turbulent and MHD turbulent flow *(for color image see journal website)*

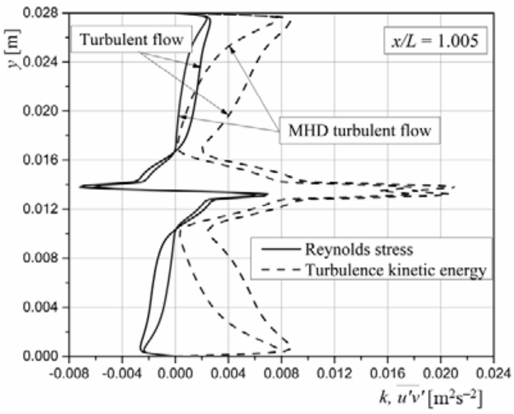

Figure 17. Turbulence kinetic energy and Reynolds stresses in wake region *(for color image see journal website)*

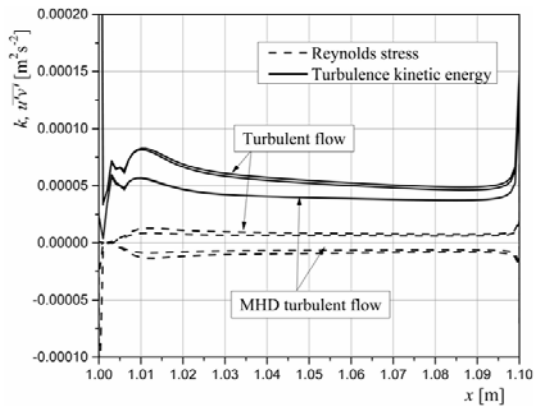

Figure 18. Turbulence kinetic energy and Reynolds stress along the flat plate *(for color image see journal website)*

In figs. 15 and 16 the velocity distribution in the boundary layer is presented. Figure 15 shows the results in the boundary layer separation zone, while the fig. 16 refers to the results obtained in sections $x/L = 0.25$ and $x/L = 0.7$. The results for MHD flow show reducing of the back flow intensity in the boundary layer separation zone, while in all other sections velocity in boundary layer is increased and free stream velocity is achieved faster.

Figures 17-22 show the influence of magnetic field on the characteristic properties of turbulent flow. All results are displayed along the polyline that was formed as a cross section of plane perpendicular to the flat plate and flat plate itself. The results show that the magnetic field has the potential to achieve reductions in the vorticity, turbulent kinetic energy, turbulence eddy dissipation, and wall shear. Diverse phenomena, such as the delay of the transition to turbulence, the selective suppression of turbulence, the reduction of boundary layer thickness, and the reduction of drag have all been observed in MHD flows.

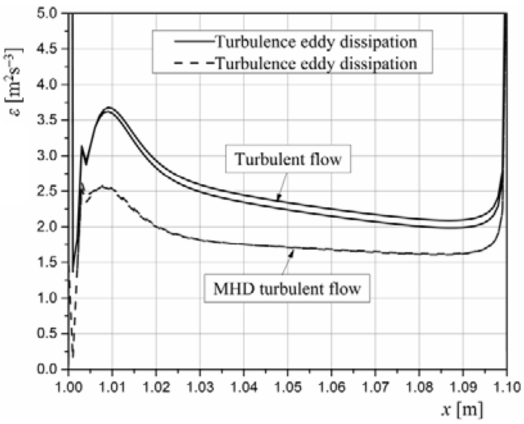

Figure 19. Turbulence eddy dissipation along the flat plate *(for color image see journal website)*

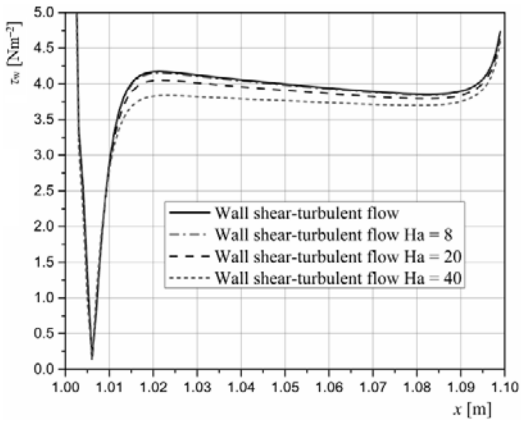

Figure 20. Wall shear along the flat plate *(for color image see journal website)*

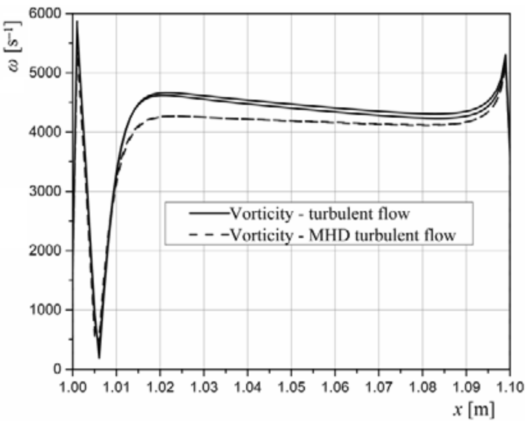

Figure 21. Vorticity along the flat plate *(for color image see journal website)*

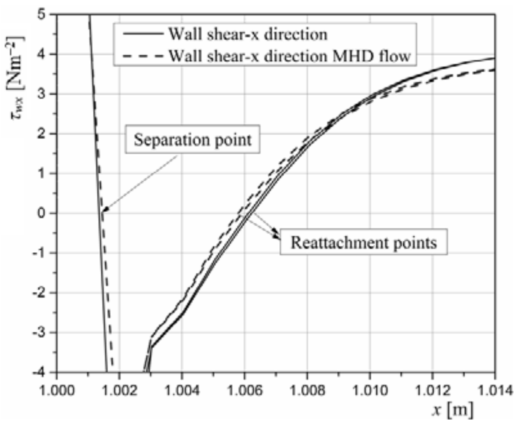

Figure 22. Wall shear in separation zone *(for color image see journal website)*

Conclusions

The present study has been undertaken to understand the effects of a magnetic field on laminar, turbulent 2-D channel flow and on flow around the flat plate. The main effect of the magnetic field *i. e*. Lorentz force, which result from the induced electric currents is to diffuse momentum along the magnetic field lines. In the case of magnetic field action flow structures tend to become elongated along this direction. According to the obtained results, documented effects range from a reduction in: turbulence kinetic energy and Reynolds stresses along the plate and in the wake, streamwise turbulent fluctuations and extensive stretching and thinning of the boundary layer. These effects have the potential to achieve reductions in the vorticity accompanying turbulence and may allow reduction of overall drag.

Acknowledgment

The research work is funded by Ministry of Education, Science, and Technological Development of Republic of Serbia through Technological Development Project no. 35016.

Nomenclature

B – magnetic field vector, [T]
F_1 – blending function, [–]
Ha – Hartmann number, [–]
j – current density vector, [Am^{-2}]
k – turbulent kinetic energy, [m^{2}s^{-2}]
Re – Reynolds number, [–]
$\mathrm{Re_m}$ – Reynolds magnetic number, [–]
II_S – shear strain rate, [s^{-1}]
U – mean velocity, [ms^{-1}]
u_i – instantaneous velocity, [ms^{-1}]
u', v' – velocity fluctuations, [ms^{-1}]
x – longitudinal coordinate [m]
y – transversal coordinate [m]

Greek symbols

β – closure coefficient, [–]
ε – turbulent dissipation rate, [m^{2}s^{-3}]
λ_{ci} – swirling strength, [s^{-1}]
μ – dynamic viscosity, [Nsm^{-2}]
μ_0 – magnetic permeability, [NA^{-2}]
μ_{t} – dynamic eddy viscosity, [Nsm^{-2}]
ν – kinematic viscosity, [m^{2}s^{-1}]
ω – specific turbulence dissipation, [s^{-1}]
ρ – fluid density, [kgm^{-3}]
σ – fluid electrical conductivity, [Sm^{-1}]
τ_{w} – wall shear, [kgm^{-1}s^{-2}]

References

[1] Laufer, J., Investigation of Turbulent Flow in a Two Dimensional Channel, NACA Rep. 1053, 1951
[2] Comte-Bellot, G., Turbulent Flow between Two Parallel Walls (in French), Ph. D. thesis, University of Grenoble (in English as ARC 31609), FM 4102, Grenoble, France, 1963
[3] Clark, J. A., A Study of Incompressible Turbulent Boundary Layers in Channel Flow, *Journal of Basic Engineering*, *90* (1968), 4, pp. 455-467
[4] Bond, D., Green is for Go, *Aviation Week & Space Technology*, *19* (2007), Aug., pp. 52-55
[5] Gad-el-Hak, M., Interactive Control of Turbulent Boundary Layers: A Futuristic Overview, *AIAA Journal*, *32* (1994), Sep., pp. 1753-1765
[6] Speziale, C. G., Analytical Methods for the Development of Reynolds-Stress Closures in Turbulence, *Annual Review of Fluid Mechanics*, *23* (1991), Jan., pp. 107–157
[7] Miner, E. W., *et al*., Examination of Wall Damping for the k-ε Turbulence Model Using Direct Simulation of Turbulent Channel Flow, *International Journal for Numerical Methods in Fluids*, *12* (1991), Apr., pp. 609-624
[8] Smolentsev, S., *et al*., Application of the *k*-*ε* Model to Open Channel Flows in a Magnetic Field, *International Journal of Engineering Science*, *40* (2002), Mar., pp. 693-711
[9] Vorobev, A., *et al.*, Anisotropy of Magnetohydrodynamic Turbulence at Low Magnetic Reynolds Number, *Physics of Fluids*, *17* (2005), 12, pp. 125105/1-125105/12
[10] Gad-El-Hak, M., Control of Low Speed Airfoil Aerodynamics, *AIAA Journal*, *28* (1990), 9, pp. 1537-1552
[11] Choi, H., *et al*., Active Turbulence Control for Drag Reduction in Wall-Bounded Flows, *Journal of Fluid Mechanics*, *262* (1994), Oct., pp. 75-110
[12] Ho, C., *et al*., Review: MEMS and Its Applications for Flow Control, *Journal of Fluids Engineering*, *118* (1996), 3, pp. 437-447
[13] Davidson, P. A., Magnetohydrodynamics in Materials Processing, *Annual Review of Fluid Mechanics*, *31* (1999), Jan., pp. 273-300
[14] Gelfgat, Yu., *et al*., On Possible Simultaneous Heating and Stirring of the Melt at Single Crystal Growth by One Inductor of Electromagnetic Field, *Magnetohydrodynamics*, *39* (2003), 2, pp. 201-210
[15] Barleon, L., *et al*., Magnetohydrodynamic Heat Transfer Research Related to the Design of Fusion Blankets, *Fusion* Technolog, *39* (2001), 2, pp. 127-156
[16] Sommeria, J., *et al*., Why, How and When MHD Turbulence Becomes Two-Dimensional, *Journal of Fluid Mechanics*, *118* (1982), May, pp. 507–518
[17] Henoch, C., Stace, J., Experimental Investigation of a Salt Water Turbulent Boundary Layer Modified by an Applied Streamwise Magnetohydrodynamic Body Force, *Physics of Fluids*, *7* (1995), 6, pp. 1371-1383
[18] Weier, T., *et al*., Boundary Layer Control by Means of Wall Parallel Lorentz Forces, *Magnetohydrodynamics*, *37* (2001), June, pp. 177-186

[19] Branover, H., *et al*., Quasi-2D Turbulence in MHD and Geophysical Flows, *Proceedings*, Second Conference on Energy Transfer in Magnetohydrodynamics Flows, 1994, Vol. 2, pp. 777–785
[20] Smolentsev, S., Moreau, R., Modeling Quasi-Two-Dimensional Turbulence in MHD Duct Flows, *Proceedings*, 2006 Summer Program, Center for Turbulence Research, Stanford University, Stanford, CA, USA, 2006, Dec., pp. 419–430
[21] Eckert, S., *et al*., MHD Turbulence Measurements in a Sodium Channel Exposed to a Transverse Magnetic Field, *International Journal of Heat and Fluid Flow*, *22* (2001), 3, pp. 358–364
[22] Pothérat, A., Alboussière, T., Small Scales and Anisotropy in Low-Rm MHD Turbulence, *Physics of Fluids*, *15* (2003), 10, pp. 1370–1380
[23] Pothérat, A., Alboussière, T., Bounds on the Attractor Dimension for Low-Rm Wall-Bound MHD Turbulence, *Physics of Fluids*, *18* (2006), 12, pp. 125102/1-125102/12
[24] Knaepen, B., Moreau, R., Magnetohydrodynamic Turbulence at Low Magnetic Reynolds Number, *Annual Review of Fluid Mechanics*, *40* (2008), pp. 25–45
[25] Spalart, P.R, *et al*., Comments on the Feasibility of LES for Wings, and on a Hybrid RANS/LES Approach, 1st AFOSR Int. Conf. On DNS/LES, Aug. 4-8, Ruston, LA, In Advances in DNS/LES, C. Liu & Z. Liu Eds., Greyden Press, Colombus, OH, USA, 1997, pp. 137-147
[26] Davidson, P. A., *An Introduction to Magnetohydrodynamics*, Cambridge University Press, Cambridge, UK, 2001

Paper submitted: August 22, 2016
Paper revised: November 24, 2016
Paper accepted: February 5, 2017